EU contract number RII3-CT-2003-506395 CARE-Report-07-028-HIPPI

A NOVEL NON-INTERCEPTING BUNCH SHAPE MONITOR FOR THE HIGH CURRENT LINAC AT GSI

Peter Forck and Christoph Dorn

GSI, Darmstadt, Germany

Abstract

For bunch length determination in the range of 0.1 to 5 ns at the GSI heavy ion LINAC a novel, non-intercepting device has been realized. It uses the time spectrum of secondary electrons created by atomic collisions between beam ions and residual gas molecules. These electrons are accelerated by an electric field of 420 V/mm toward an electro-static energy analyzer, which is used to restrict the effective source region. Then the electrons are deflected by an rf-resonator running in phase with the acceleration frequency (36 or 108 MHz) to transform the time spectrum into spatial separation. The detection is done with a 70 mm diameter Micro Channel Plate. First tests were performed and it was shown that the achieved time resolution is about 50 ps, corresponding to 2 degree of the accelerating 108 MHz phase.

Introduction

The determination of the longitudinal density distribution of a bunched beam is an important issue because it is required for an optimal matching between different LINAC-modules as well as for the comparison with numerical calculations also taking space charge effects into account. Measurements of this parameter are much less often performed compared to their transverse counterpart, the transverse profile due to the relatively complex instrumentation required. In a several case non-Gaussian longitudinal profiles were observed. At proton and ion LINACs the bunch structure cannot be determined by capacitive pick-ups due to the non-relativistic beam velocities ($\beta < 20$ % at the GSI-LINAC) causing a faster propagation of the electric field of bunches. At most LINACs the bunch structure is determined by secondary electrons emitted from a wire crossing the beam [1,2,3]. The wire is biased to about -10 kV to pull the secondary electrons toward a slit outside the beam path. An rf-deflector follows, where the electrons are modulated in transverse direction by an electric rf-field. The deflection angle depends on their relative phases, i.e. the device transforms the time information into a spatial distribution.

For the high current beam operation at GSI with heavy ions and currents up to 20 mA [4], the beam power is sufficient to melt intersecting materials. The above mentioned wire-based principle is adapted to a non-intersecting device by performing the time spectroscopy of secondary electrons created by atomic collisions between beam ions and residual gas molecules. The electrons are accelerated by a homogeneous electrical field formed by electrodes outside of the beam pass, as usually used for Ionization Profile Monitors. To restrict the source region for the secondary electrons, an aperture system and an electro-static energy analyzer is used. The time-to-spatial transformation is performed with an rf-deflector developed at INR, Moscow [3]. As the electron detector we used a large Micro Channel Plate MCP connected to a phosphor screen and observed by a CCD camera. Numerical calculations of the expected resolution and detailed tests of the novel device are reported here. It can serve as a prototype for the determination of the bunch-length at LINACs designed within the HIPPI project.

Monitor hardware

The schematic layout of the monitor is displayed in Fig. 1: At the detector location, the beam passes a static electric field region generated by a $160\text{x}60\text{mm}^2$ electrode biased up to -30 kV. With the help of field forming strips, a homogeneous field of 420 V/mm perpendiculars to the beam direction guides the secondary electrons toward a grounded plate with a horizontal slit of 1.5 mm in beam direction. The relatively complex mechanical realization is shown in Fig. 2. To shorten the source length Δz in beam direction and the corresponding divergence of the secondary electron beam, two apertures with a distance of 70 mm are used. Their opening can be varied remotely between 0.1 and 2 mm by dc-motors. The second aperture serves as entrance slit of a 90^0 cylindrical electro-static energy analyzer with a bending radius of ρ_0=30 mm. The nominal voltages are ±5.5 kV for the opposite cylinder segments. Two similar devices are installed to place the electron detector perpendicular to the beam pipe. A third aperture is located 10 mm downstream from the second cylinder edge to enable a point-to-point focusing from the entrance- to the exit-slit [4]. Using ±0.25 mm opening for aperture 1 and 2 as well as ±0.5 mm for aperture 3, the vertical source prolongation is restricted to about $\Delta y = \pm 0.2$ mm (see below), which is comparable to the wire thickness in the standard method [1].

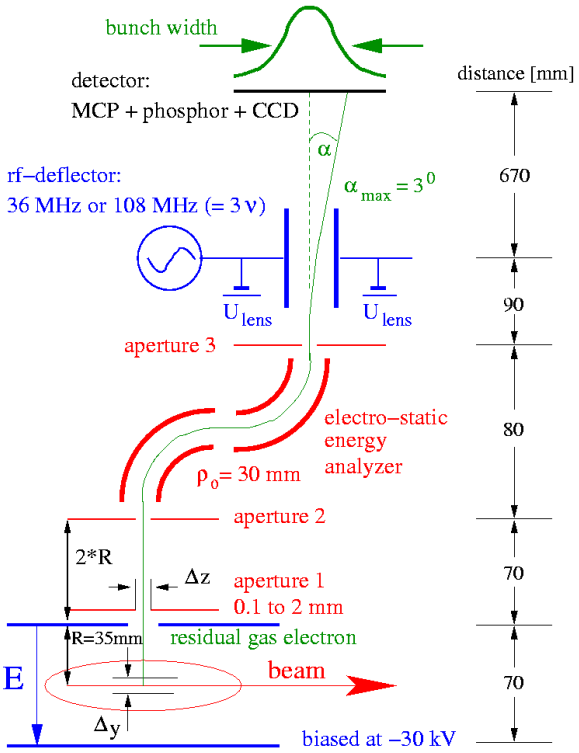

Figure 1: Schematic sketch of the bunch shape monitor.

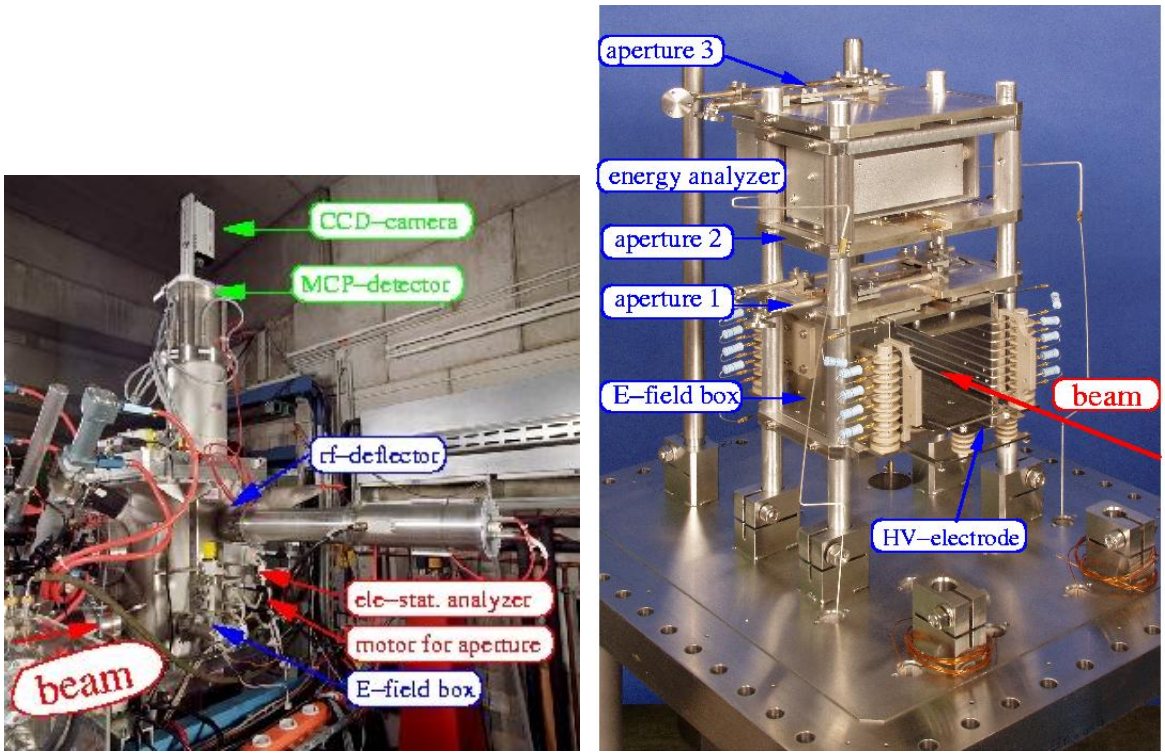

Figure 2: Left: The installation at the target location**.** ***Right:*** Photo of the electric field box and the energy analyser, mounted on a rectangular flange of 340x400 mm^2 and installed at the bottom of the vacuum chamber. The opening for the beam is 70x70 mm^2.

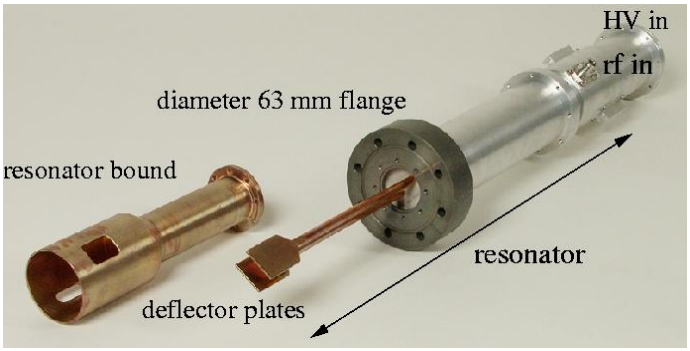

Figure 3: The 108 MHz rf-deflector with removed housing is shown.

After a drift of 90 mm the time information is transferred into spatial distribution by the rf-deflector synchronized with the LINAC rf, see Fig. 3. Two types of rf-deflectors are available, one running at the base-frequency of 36 MHz for the measurement of long bunches and one for short bunches at the third harmonics at 108 MHz. The deflectors are built as 800 mm long parallel-wire $\lambda/4$-resonators [3] having a quality factor of Q_0=290 and Q_0= 370 for the 36 and 108 MHz device, respectively. The 108 MHz type has straight parallel-wires, while spiralled wires are used for the 36 MHz device. The maximum rf-power fed into the resonator is 100 W and 50 W for the 36 MHz and 108 MHz, respectively. This power leads to a maximum deflection angle $\alpha_{max}=3^0$. A 6 ms pulse length for the rf-power is sufficiently longer than the maximum macro beam pulse. The parallel wires of the rf-deflector are also used as a focusing element by biasing them with maximal voltage U_{lens}=-7 kV acting as an electro-static einzel-lens. On top of the focusing voltage, a different biasing of the plates is used for steering of the electron beam. After a flight path of 670 mm these single electrons are detected by a 70 mm diameter Chevron MCP (Hamamatsu F2226-24P) equipped with a P20 phosphor screen. The light spots are read out with a 12 bit digital CCD camera (PCO SensiCam) having a 480x640 pixel VGA-resolution and a fibre optic link for digital data communication.

Beam based measurements

Systematic test measurements at a target location were performed at 11.4 MeV/u for several ion beams. Without applying rf-power to the deflector the optics of the energy analyzer was checked. As shown in Fig. 4 the electron beam can be focused by the einzel-lens functionality of the defector. On the MCP and a spot size of 1 mm can be reached, which corresponds to about 6 pixels. This coincides with the optical calculations for the nominal aperture settings of the energy analyzer. Due to the 70 mm active diameter of the MCP this width contributes by only a few % to the monitor resolution depending on the rf-power applied to the rf-deflector. For the measurements of Fig. 5 and 6 it corresponds to a time resolution of about 50 ps. A smaller aperture opening can even reduce the beam spot size, but then also the signal strength decreases.

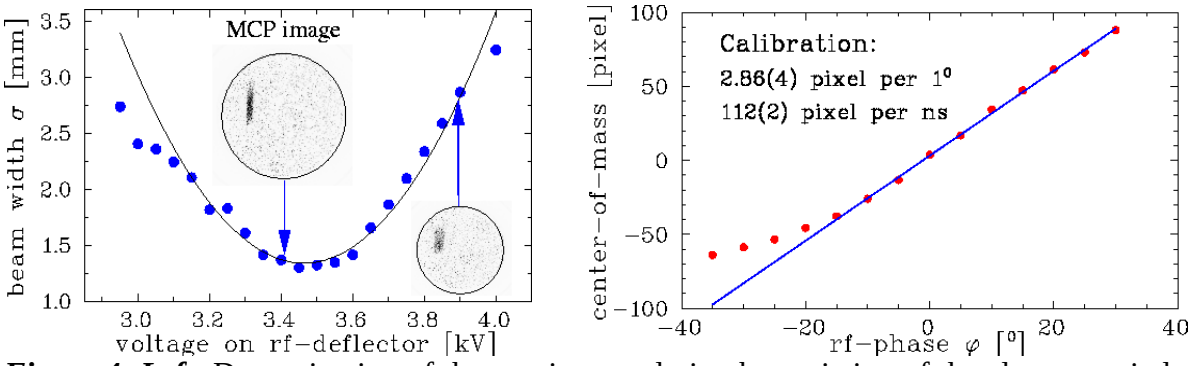

Figure 4: Left: Determination of the monitor resolution by variation of the electro-static lens voltage without applying rf to the deflector for the nominal aperture setting of ±0.25 mm for aperture 1 and 2 and ±0.5 mm for aperture 3. ***Right:*** The central position of the bunch is determined as a function of the relative phase shift to prove the linearity and serve as a calibration between measured CCD pixels and the absolute time or phase difference.

To illuminate the full MCP, the rf-power of the rf-deflector can be varied. Therefore, quite different bunch lengths can be measured. A calibration of the bunch centre position at the MCP with respect to the rf-phase is required to achieve an absolute time or phase scale. An example is shown in Fig. 4 using a digital rf-phase shifter with ~0.3^0 accuracy. In addition, the plots prove the linearity of the transverse deflection as long as the rf-phase difference between deflection voltage and the bunch stays within an interval of ~45^0. For large phase differences, the non-linear behaviour of the sine-wave starts to contribute.
A typical raw image of the bunch as recorded by the CCD camera is shown in Fig. 5. The deflection with a frequency of 108 MHz is displayed horizontally spanning 3.6 ns. The projection of the light intensity on this axis gives the bunch shape. This measurement proves the general functionality of this novel device. Short bunches down to σ = 125 ps were monitored during the test installation.

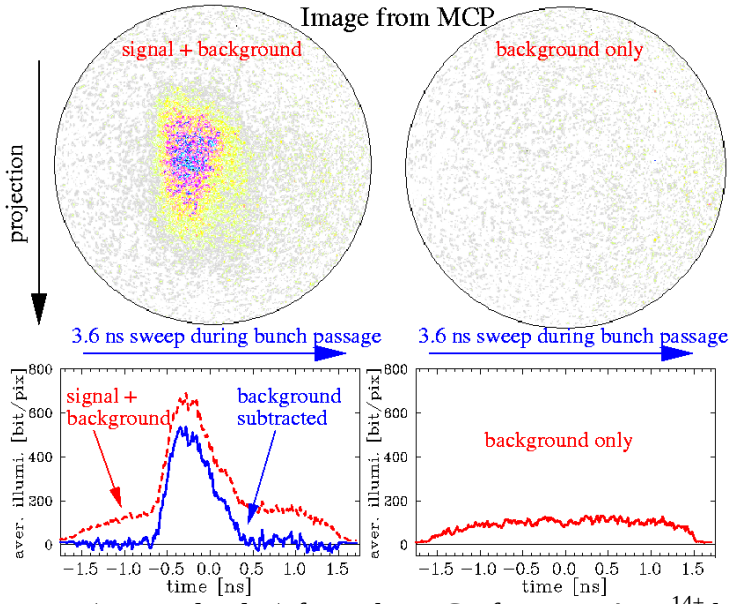

Figure 5: Typical image (inverted color) from the MCP for a 2 mA Ni^{14+} beam averaged over 8 macro-pulses with 0.2 ms duration and a vacuum pressure of $2x10^{-6}$ mbar. 15 W had been fed to the 108 MHz rf-deflector.

It is required to subtract a homogeneous distributed background. This background is only present during beam delivery and is not influenced by the aperture opening. Presently, its

origin is not well understood. It might be due to x-rays from secondary electrons accelerated by the electric field and hitting the stainless steel plate of the electric field box. But the installation of a 5 mm thick steel shielding behind the energy analyzer for x-ray absorption (maximum energy 30 keV) did not lead to a significant reduction. A biased grid close to the HV-electrode was installed to prevent for secondary electrons entering the interaction region. But no significant reduction of the background was observed. Another reasons for the background might be neutrons or γs emitted at the nearby beam dump at the target location for the tests, see Fig. 1. A nearly background-free measurement is intended to allow single macro-pulse monitoring. Moreover, with an enhanced signal quality, a smaller aperture opening can increase the monitor resolution and possible non-Gaussian bunch-structure contributions can be detected within a single macro-pulse. The image of the bunch can then be spread over the full MCP area and a resolution down to ~20 ps would be achievable.
The displayed measurement had been performed with a high current setting of 2 mA Ni^{14+} beam. But the same signal quality can be reached for low current settings. If the amount of secondary electrons does not result in a sufficient statistic, the vacuum pressure can be raised by a regulated gas inlet system. It has been proved that a local pressure bumps up to 10^{-4} mbar in the transfer lines at GSI does not influence the beam properties. Due to the statistical nature, averaging also improves the signal-to-noise ratio leading to a large dynamic range.
An application of the bunch shape monitor is to determine the longitudinal emittance. By varying the voltage amplitude of a buncher cavity and measuring the bunch width, the longitudinal emittance in a linear approximation can be calculated by fitting a parabola through the square of the bunch width, as displayed in Fig. 6.

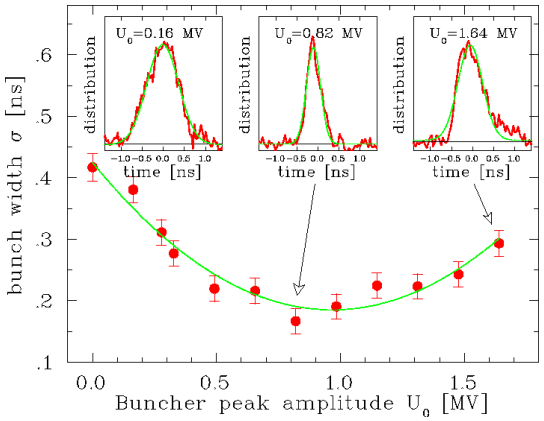

Figure 6: Measurement of the bunch width (one standard deviation) as a function of the buncher voltage 31 m upstream of the detector is performed with the same beam as of Fig. 5.

Numerical calculations in the presence of space charge

Compared to the 'standard' method by an intercepting wire [1] a larger contribution for the bunch space charge is expected for the following reason: Close to the wire the electric field for the secondary electron acceleration is large, while for our setup the electric field is constant during the whole acceleration process. Therefore, the influence of the beam's electric space-charge field on the detected electrons is of importance. A numerical analysis is required to estimate the beam current and bunch length, where the electron trajectories are deformed significantly, resulting in a misleading signal reading.
As a model for bunches, a parabolic charge distribution was used. For an equal transverse, but arbitrary longitudinal prolongation, the electric field of the moving bunches can be given analytically [7]. Using a Runge-Kutta scheme the secondary electrons are tracked with a time resolution of 0.3 ps per step through bunch field and the homogeneous E-field region toward aperture 1 in Fig. 1. From thereon linear optics are adequate for the action of the electro-static

analyzer and related drift spaces. The three-dimensional start co-ordinates and velocities for the secondary electrons are chosen by a Monte-Carlo simulation satisfying the given distribution functions. For the initial velocities, a realistic distribution function for the `δ-electrons' [8] was used with maximal electron energy of 100 eV. Varying this cut-off energy has only a small influence on the signal shape, because most electrons are emitted with lower energies.

We discuss the essential features for the case of the reported measurements shown in Fig. 6 having a beam current of 2 mA and a bunch length of σ=0.2 ns. Three plots are presented in Fig. 7 to characterize the functionality for the device. Because of the beam space-charge driving forces, a beam current dependence is expected and we compare a low current case (the space charge field is much below the external field strength), a medium case, where the measurements are done and a case above the maximum expected ion currents for the GSI LINAC.

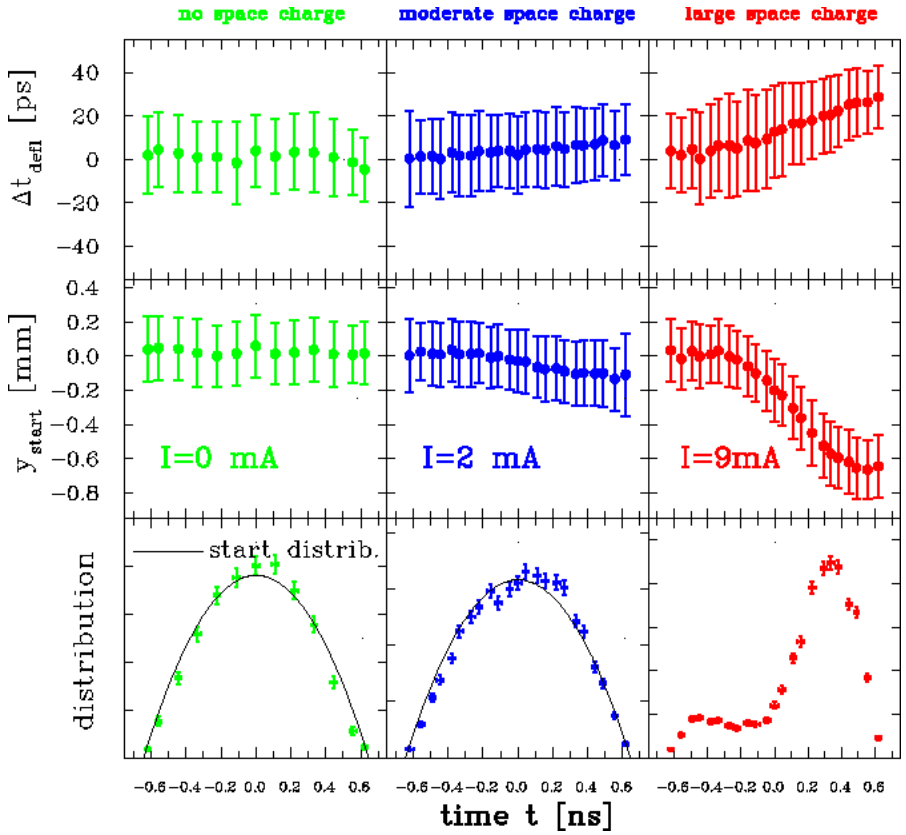

Figure 7: Simulation for a parabolic bunch shape at 11.4 MeV/u, 36 MHz repetition rate and a transverse parabolic beam size of ±5 mm root points is presented. The left column shows the simulation low current, the middle for 2 mA current (as for the reported measurements) and the right column for 9 mA. ***Top:*** arrival time Δt_{defl} at the rf-deflector with respect to the reference particle. ***Middle:*** vertical start co-ordinate y_{start}; the error bars are the standard deviation of the ensemble. ***Bottom:*** Number of detected electrons; vertical error bars given by the square root of the number, horizontal error bars are the ensemble standard deviation of the arrival time.

The first row in Fig. 7 shows the time resolution, i.e. the spread of the arrival times as a function of time during the bunch passage (Fig. 7 top). For the low and medium current range of 2 mA this time spread remains ±20 ps without significant shifts along the bunch. The second quantity is the spread of the initial position along the bunch (Fig. 7 middle). For the 2 mA case, the detected particles are created within ±0.2 mm, with a slight decrease by 0.2 mm at the bunch head. The third quantity is the number of detected electrons as a function of

bunch position, which corresponds directly to experimentally determined signal strength (Fig. 7 bottom). There is no deformation for the low current case and only a small deformation around the bunch centre for the medium case, which is below the required signal accuracy. This proves the right signal reading and resolution for those parameters.
With a current increased to 9 mA the time resolution is slightly worse: Secondary electrons created by the bunch head arrive ~30 ps earlier (Fig. 7 top). Those electrons are created ~0.6 mm below the bunch centre (Fig. 7 middle). This is tolerable due to the transverse beam width of σ= 2.3 mm and the lack of a vertical-longitudinal coupling. However, the number of detected electrons as a function of the bunch position shows a maximum at the bunch head (Fig. 7 bottom). This can qualitatively explained by the electric field at the bunch head, which pulls the secondary electrons toward the bunch centre. These electrons are influenced during their full passage of ~1.1 ns toward aperture 1. For the secondary electrons from the bunch tail, this strong force acts in a shorter time because the bunch departs from the active detector volume. This limits the applicability of the present device in case of very short and intense bunches.

Conclusion

A novel, non-intersecting device for the bunch structure determination has been successfully tested. It can be used in a wide current range and offers a direct determination of parameters that are difficult to measure. For high currents and moderate bunch-length in the ns range, the bunch structure is reproduced faultlessly. Only for very high intensities, the beam's space charge influence on the secondary electrons trajectory significantly. Presently, the origin of the diffuse background is not well understood and limits the achievable resolution. After it's reducing a high-resolution single macro-pulse observation seems to be possible. However, one has to state that the complex mechanical realization and its control do not allow a routine operation at the present stage. Moreover, detailed calculations are required concerning the beam's space charge contribution as well as understanding the origin of the background. These improvements will be performed in near future by additional personnel and detailed beam-based tests.

Acknowledgements

We like to thank, H. Graf, M. Herty, P. Strehl from GSI, A. Feschenko, V. Peplov from INR as well as S. Sharamentov from ANL for valuable discussion and the technical realization. We acknowledge the support of the European Community-Research Infrastructure Activity under the FP6 "Structuring the European Research Area" programme (CARE, contract number RII3-CT-2003-506395).

References

[1] A. Feschenko, *Proc. PAC 2001, Chicago*, p. 517 (2001) and references therein.
[2] N.E. Vinogradov et al., *Nucl. Instrum. Meth.*, **A 526**, p. 206 (2004), N.E. Vinogradov et al., *Proc. XXI LINAC, Gyeongju*, p. 61 (2002).
[3] Y.V. Bylinsky et al., *Proc. EPAC 1994, London*, p 1702 (1994).
[4] W. Barth et al., *Proc. PAC 2001, Chicago*, p. 3281 (2001), W. Barth et al, *Proc. XX LINAC Conf. 2000, Monterey*, p. 1033 (2000).
[5] See e.g. H. Wollnik, *Optics of Charged Particles*, Academic Press (1987).
[6] P. Forck et al., *Proc. EPAC 2005, Lucerne*, p. 2541 (2004).
[7] P. Strehl, *Beam Instrumentation and Diagnostics*, Springer Verlag (2006).
[8] See e.g. *Secondary Electron Spectra from Charge Particle Interaction*, ICRU Report 55 (1996).